

Graph fission in an evolving voter model

Richard Durrett^{a,1}, James P. Gleeson^b, Alun L. Lloyd^{c,d}, Peter J. Mucha^e, Feng Shi^e, David Sivakoff^a, Joshua E. S. Socolar^f, and Chris Varghese^f

^aDepartment of Mathematics, Duke University, Box 90320, Durham, NC 27708; ^bMathematics Applications Consortium for Science and Industry, Department of Mathematics and Statistics, University of Limerick, Limerick, Ireland; ^cDepartment of Mathematics, Box 8205, North Carolina State University, Raleigh, NC 27695-8205; ^dFogarty International Center, National Institutes of Health, Bethesda, MD 20892; ^eDepartment of Mathematics, CB 3250, University of North Carolina, Chapel Hill, NC 27599; and ^fDepartment of Physics, Duke University, Box 90305, Durham, NC 27708

Contributed by Richard T. Durrett, January 13, 2012 (sent for review October 26, 2011)

We consider a simplified model of a social network in which individuals have one of two opinions (called 0 and 1) and their opinions and the network connections coevolve. Edges are picked at random. If the two connected individuals hold different opinions then, with probability $1 - \alpha$, one imitates the opinion of the other; otherwise (i.e., with probability α), the link between them is broken and one of them makes a new connection to an individual chosen at random (i) from those with the same opinion or (ii) from the network as a whole. The evolution of the system stops when there are no longer any discordant edges connecting individuals with different opinions. Letting ρ be the fraction of voters holding the minority opinion after the evolution stops, we are interested in how ρ depends on α and the initial fraction u of voters with opinion 1. In case (i), there is a critical value α_c which does not depend on u , with $\rho \approx u$ for $\alpha > \alpha_c$ and $\rho \approx 0$ for $\alpha < \alpha_c$. In case (ii), the transition point $\alpha_c(u)$ depends on the initial density u . For $\alpha > \alpha_c(u)$, $\rho \approx u$, but for $\alpha < \alpha_c(u)$, we have $\rho(\alpha, u) = \rho(\alpha, 1/2)$. Using simulations and approximate calculations, we explain why these two nearly identical models have such dramatically different phase transitions.

coevolutionary network | quasi-stationary distribution | Wright–Fisher diffusion | approximate master equation

In recent years, a variety of research efforts from different disciplines have combined with established studies in social network analysis and random graph models to fundamentally change the way we think about networks. Significant attention has focused on the implications of dynamics in establishing network structure, including preferential attachment, rewiring, and other mechanisms (1–5). At the same time, the impact of structural properties on dynamics on those networks has been studied, (6), including the spread of epidemics (7–10), opinions (11–13), information cascades (14–16), and evolutionary games (17, 18). Of course, in many real-world networks the evolution of the edges in the network is tied to the states of the vertices and vice versa. Networks that exhibit such a feedback are called adaptive or coevolutionary networks (19, 20). As in the case of static networks, significant attention has been paid to evolutionary games (21–24) and to the spread of epidemics (25–29) and opinions (30–35), including the polarization of a network of opinions into two groups (36, 37). In this paper, we examine two closely related variants of a simple, abstract model for coevolution of a network and the opinions of its members.

Holme–Newman Model

Our starting point is the model of Holme and Newman (38–41). They begin with a network of N vertices and M edges, where each vertex x has an opinion $\xi(x)$ from a set of G possible opinions and the number of people per opinion $\gamma_N = N/G$ stays bounded as N gets large. On each step of the process, a vertex x is picked at random. If its degree $d(x) = 0$, nothing happens. For $d(x) > 0$, (i) with probability α an edge attached to vertex x is selected and the other end of that edge is moved to a vertex chosen at random from those with opinion $\xi(x)$; (ii) otherwise (i.e., with probability $1 - \alpha$) a random neighbor y of x is selected and we

set $\xi(x) = \xi(y)$. This process continues until there are no longer any edges connecting individuals with different opinions.

When $\alpha = 1$, only rewiring steps occur, so once all of the M edges have been touched, the graph has been disconnected into G components, each consisting of individuals who share the same opinion. Because none of the opinions have changed, the components are small (i.e., their sizes are Poisson with mean γ_N). By classical results for the coupon collector's problem, this requires approximately $M \log M$ updates (see, e.g., ref. 42, p. 57).

In contrast, for $\alpha = 0$, this system reduces to the voter model on a static graph. If we suppose that the initial graph is an Erdős–Rényi random graph in which each vertex has average degree $\lambda > 1$, then (see, e.g., ref. 12, chap. 2) there is a “giant component” that contains a positive fraction, μN , of the vertices and the second largest component is small having only $O(\log N)$ vertices; i.e., when N is large, the size will be approximately $C_\lambda \log N$, where C_λ is a constant that depends on λ . The voter model on the giant component will reach consensus in $O(N^2)$ steps (see, e.g., ref. 12, sect. 6.9), so the end result is that one opinion has μN followers while all of the other groups are small.

Using simulation and finite size scaling, Holme and Newman showed that there is a critical value α_c so that for $\alpha > \alpha_c$ all of the opinions have a small number of followers at the end of the process, whereas for $\alpha < \alpha_c$ “a giant community of like-minded individuals forms” (38). When the average degree $\lambda = 2M/N = 4$ and the number of individuals per opinion $\gamma_N \rightarrow 10$, this transition occurs at $\alpha_c \approx 0.46$.

Our Model and Simulation Results

The “rewire-to-same” model we study differs from that of Holme and Newman in two ways: (i) we consider two opinions (called 0 and 1) instead of a number proportional to the size of the graph; and (ii) on each step, we pick a discordant edge (x, y) at random rather than a vertex, avoiding the problem of picking vertices with degree zero or vertices that agree with all of their neighbors. With probability $1 - \alpha$, the voter at x adopts the opinion of the voter at y . Otherwise (i.e., with probability α), x breaks its connection to y and makes a new connection to a voter chosen at random from those that share its opinion. The process continues until there are no edges connecting voters that disagree.

Despite the differences in implementation, this rewire-to-same model has a phase transition similar to that of Holme and Newman. In particular, the final fraction ρ of voters with the minority opinion undergoes a discontinuous transition at a value α_c that does not depend on the initial density. Fig. 1 shows results of simulations for the rewire-to-same model starting from an initial graph that is Erdős–Rényi with $N = 100,000$ vertices and average degree $\lambda = 4$. Opinions are initially assigned randomly with the

Author contributions: R.D., J.P.G., A.L.L., P.J.M., F.S., D.S., J.E.S.S., and C.V. performed research; and R.D. and P.J.M. wrote the paper.

The authors declare no conflict of interest.

Freely available online through the PNAS open access option.

¹To whom correspondence should be addressed. E-mail: rtd@math.duke.edu.

This article contains supporting information online at www.pnas.org/lookup/suppl/doi:10.1073/pnas.1200709109/-DCSupplemental.

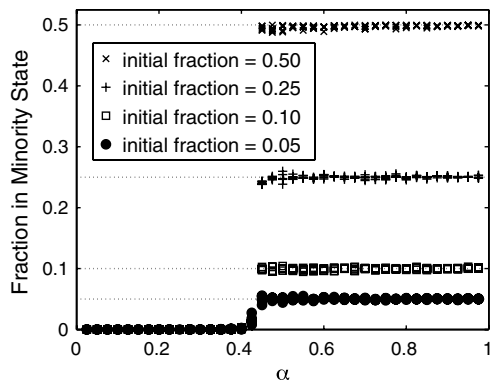


Fig. 1. Simulation results for rewired-to-same model, starting from Erdős-Rényi graphs with $N = 100,000$ nodes and average degree $\lambda = 4$.

probability of opinion 1 given by $u = 0.5, 0.25, 0.1$, and 0.05 . The figure shows the final fraction ρ of voters with the minority opinion from five realizations for each u . For $\alpha > \alpha_c \approx 0.43$, we observe $\rho \approx u$ and for $\alpha < \alpha_c$, $\rho \approx 0$.

We also study a “rewired-to-random” variant of this model that differs from the rewired-to-same model in only one way: x makes its new connection to a voter chosen at random from all of the vertices in the graph. This single difference leads to fundamentally different model outcomes, as seen in Fig. 2, showing simulation results for the rewired-to-random model on initially Erdős-Rényi graphs with $N = 100,000$ nodes and average degree $\lambda = 4$ for $u = 0.5, 0.25, 0.1$, and 0.05 . When $u = 0.5$, the fraction in the minority is constant at 0.5 over $[\alpha_c(0.5), 1]$ and then decreases continuously to a value near zero as α decreases to zero.

The behavior of our models for $\alpha > \alpha_c$ is easy to understand. As in the case of the Holme and Newman model, we expect consensus to be reached in $O(N \log N)$ steps when $\alpha = 1$ and in $O(N^2)$ steps when $\alpha = 0$. We define the boundary between the fast and slow consensus regimes to be the value of α , where the average number of steps needed to reach consensus is $N^{3/2}$ (any power between one and two would give the same results when $N \rightarrow \infty$). When an edge is chosen between voters with different opinions, then a rewiring event does not change the number of ones, whereas a voting event will increase and decrease the number of ones with equal probability; i.e., the number of ones is a random walk that on each step stays constant with probability α . The central limit theorem implies that when consensus is reached in $O(N^{3/2})$ steps, the typical change in the number of ones from the initial configuration is $O(N^{3/4})$. Hence, when the initial fractions of ones is $u \leq 1/2$, the final fraction ρ with the minority opinion will be approximately equal to u .

Turning to the curves in Fig. 2 for $u = 0.25, 0.1$, and 0.05 , we see that each initial density u has a critical value $\alpha_c(u)$, so that for

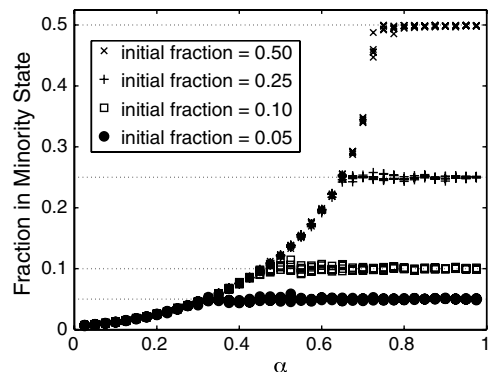


Fig. 2. Simulation results for the rewired-to-random model, starting from Erdős-Rényi graphs with $N = 100,000$ nodes and average degree $\lambda = 4$.

$\alpha > \alpha_c(u)$, we have $\rho(\alpha, u) = u$, whereas for $\alpha < \alpha_c(u)$, we have $\rho(\alpha, u) = \rho(\alpha, 0.5)$. Because all of the $\rho(\alpha, u)$ agree with $\rho(\alpha, 0.5)$ when they are $< u$, we call the graph of $\rho(\alpha, 0.5)$ on $[0, \alpha_c(0.5)]$ the universal curve. The main goal of this paper is to explain this phenomenon.

Quasi-Stationary Distributions

Let N_i be the number of vertices in state i . Our first clue to the reason for a universal curve in the rewired-to-random model came from Fig. 3, which shows the change over time of the fraction of vertices with the minority opinion $\min\{N_1, N_0\}/N$ and the number of edges connecting vertices with opposite opinions, N_{10} , for a simulation in which the initial density of ones is $u = 1/2$, $\alpha = 0.3$, the number of nodes is $N = 1,000$, and we start with an Erdős-Rényi graph with average degree $\lambda = 4$. In the visualization of these results and the theoretical discussions that follow, the model is considered in continuous time with each edge subject to change at times of a rate one Poisson process. The sequence of states visited by the model is the same in discrete or continuous time, but tM updates correspond to continuous time t . Hence, in the slow consensus regime, $O(N^2)$ updates becomes time $O(N)$.

There are $M \approx 2,000$ edges in this graph simulated in Fig. 3, so the initial number of 1-0 edges is approximately 1,000, but the curve drops very quickly to a value near 600, and then begins to change more slowly. The second key observation is that the number of 0-1 edges and the fraction with the minority opinion $\min\{N_1, N_0\}/N$ appear to be strongly correlated. The initial transient and the reason for the correlation will be seen more clearly in Fig. 4.

To explain the key insight derived from this simulation, we recall results for the voter model on the d -dimensional integer lattice \mathbb{Z}^d , in which each vertex decides to change its opinion at rate 1, and when it does, it adopts the opinion of one of its $2d$ nearest neighbors chosen at random. Let $\xi_t(x)$ be the opinion of the voter at x at time t . Holley and Liggett (43) and Liggett (44) proved the following result.

Theorem. In $d \leq 2$, the voter model approaches complete consensus; that is, if $x \neq y$ then $P[\xi_t(x) \neq \xi_t(y)] \rightarrow 0$. In $d \geq 3$, if the voter model starts from product measure with density p [i.e., $\xi_0^p(x)$ are independent and equal to one with probability p], then ξ_t^p converges in distribution to a limit ν_p , which is a stationary distribution for the voter model.

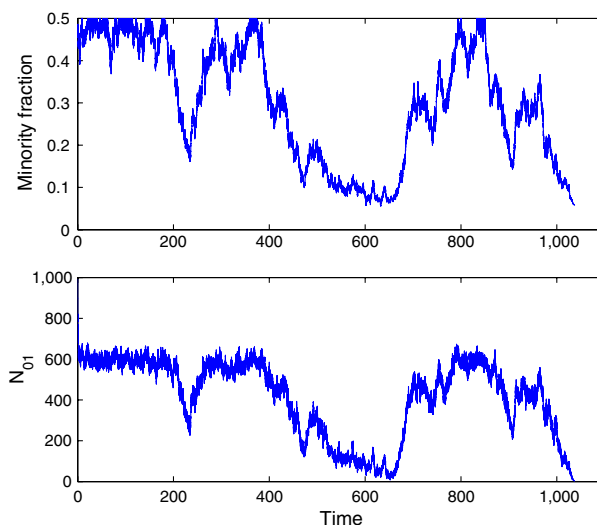


Fig. 3. Fraction of nodes with the minority opinion ($\min\{N_0, N_1\}/N$) and the number of discordant edges N_{10} versus time, for a simulation of $N = 1,000$ nodes, $u = 0.5$, and $\alpha = 0.3$.

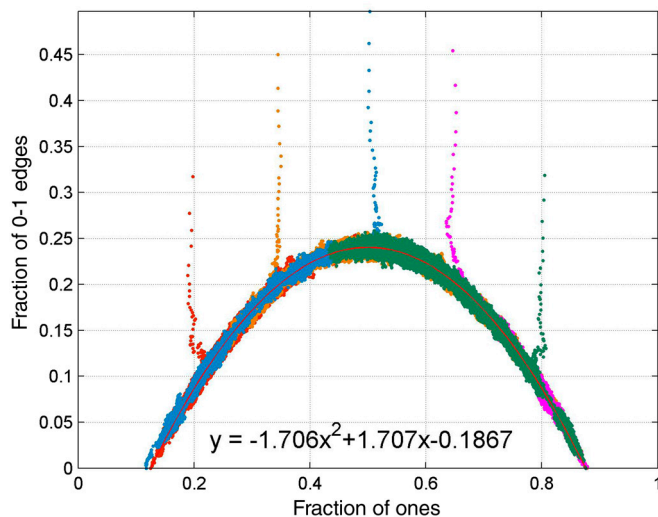


Fig. 4. Plot of N_{10}/M versus N_1/N when $\alpha = 0.5$ in the rewiring-to-random case. Five simulations starting from $u = 0.2, 0.35, 0.5, 0.65$, and 0.8 are plotted in different colors. These results are from graphs with $N = 10,000$ vertices and plotted every 1,000 steps.

Simulations of the voter model are done on a finite set, typically the torus $(\mathbb{Z} \bmod L)^d$. In this setting, the behavior of the voter model is “trivial” because it is a finite Markov chain with two absorbing states, all ones and all zeros. As the next result shows (see Cox and Greven, ref. 45), the voter model has interesting behavior along the road to absorption.

Theorem. *If the voter model on the torus in $d \geq 3$ starts from product measure with density p , then at time Nt it looks locally like $\nu_{\theta(t)}$ where the density θ_t changes according to the Wright–Fisher diffusion process*

$$d\theta_t = \sqrt{\beta_d \cdot 2\theta_t(1 - \theta_t)}dB_t$$

and β_d is the probability that two random walks starting from neighboring sites never hit.

In the next section we will describe conjectures for the evolving voter model that are analogues of the last theorem. To prepare for stating our conjectures, note that (i) although the voter model on the torus does not have a nontrivial stationary distribution, it does have a one parameter family of “quasi-stationary distributions” that look locally like ν_p , and (ii) the quantity under the square root in the Wright–Fisher diffusion is, by results of Holley and Liggett (43), the expected value of N_{10}/M under $\nu_{\theta(1)}$.

Conjectures

Our next goal is to use simulation results to formulate the analogues of the Cox and Greven result (45) for our two evolving voter models, beginning with the more interesting rewired-to-random case. Fig. 4 shows results from simulations of the system with $\alpha = 0.5$. The initial graph is Erdős–Rényi with $N = 10,000$ vertices and average degree $\lambda = 4$. Observations of the pair $(N_1/N, N_{10}/M)$ are plotted every 1,000 steps starting from densities $u = 0.2, 0.35, 0.5, 0.65$, and 0.8 . The plotted points converge quickly to a curve that is approximately (fitting to a parabola) $1.707x(1-x) - 0.1867$ and then diffuse along the curve until they hit the axis near 0.125 or 0.875 . Thus the final fraction with the minority opinion $\rho \approx 0.125$, a value that agrees with the universal curve in Fig. 2 at $\alpha = 0.5$.

The fact that, after the initial transient, N_{10}/M is a function of N_1/N supports the conjecture that the evolving voter model has a one parameter family of quasi-stationary distributions, for if this is true, then the values of all of the graph statistics can be computed from N_1/N . To further test this conjecture, we examined

the joint distribution of the opinions at three sites. Let N_{ijk} be the number of oriented triples x - y - z of adjacent sites having states i, j, k , respectively. Note for example, in the 010 case, this will count all such triples twice, but this is the approach taken in the theory of limits of dense graphs (46), where the general statistic is the number of homomorphisms of some small graph (labeled by ones and zeros in our case) into the random graph being studied.

Fig. 5 shows a plot of N_{010}/N versus N_1/N . After an initial transient, the observed values stay close to a curve that is well approximated by a cubic. Simulations of the other N_{ijk} show similar behavior. Because the numbers of 010 triples must vanish when the number of 1-0 edges do, the fitted cubic shares two roots with the quadratic approximating the graph of N_{10}/M versus N_1/N . This quadratic curve (see again Fig. 4 for $\alpha = 0.5$) is fundamental to our understanding of the observed system behavior, and we hereafter refer to it as the “arch.”

The phenomena just described for $\alpha = 0.5$ also hold for other values of α . Fig. 6 shows the arches that correspond to $\alpha = 0.1, 0.2, \dots, 0.7$. Numerical results show that the curves are well approximated by $c_\alpha u(1-u) - b_\alpha$. Let $(v(\alpha), 1-v(\alpha))$ be the “support interval” where the arch has positive values. Simulations show that if $u < v(\alpha)$, then the simulated curve rapidly goes almost straight down and hits the axis where $N_{10} = 0$.

Conjecture 1. *In the rewiring-to-random model, if $\alpha < \alpha_c(1/2)$ and $v(\alpha) < u \leq 1/2$, then starting from product measure with density u of ones, the evolving voter model converges rapidly to a quasi-stationary distribution $\nu_{\alpha,u}$. At time tN , the evolving voter model looks locally like $\nu_{\alpha,\theta(t)}$ where the density changes according to a generalized Wright–Fisher diffusion process*

$$d\theta_t = \sqrt{(1 - \alpha)[c_\alpha \theta_t(1 - \theta_t) - b_\alpha]} dB_t$$

until θ_t reaches $v(\alpha)$ or $1 - v(\alpha)$.

Here the quantity under the square root is $(1 - \alpha)N_{10}/M$ with $(1 - \alpha)$ equal to the fraction of steps that are voter steps because rewiring steps do not change the number of ones.

If Conjecture 1 is true, then the universal curve in Fig. 2 has $\rho(\alpha, 0.5) = v(\alpha)$ for $\alpha < \alpha_c(0.5)$. When α is close to $\alpha_c(0.5)$, $v(\alpha) \approx 1/2$, so when the evolving voter model hits $N_{10} = 0$ both opinions are held by large groups, and the graph splits into two giant connected components (that is, their size is proportional to

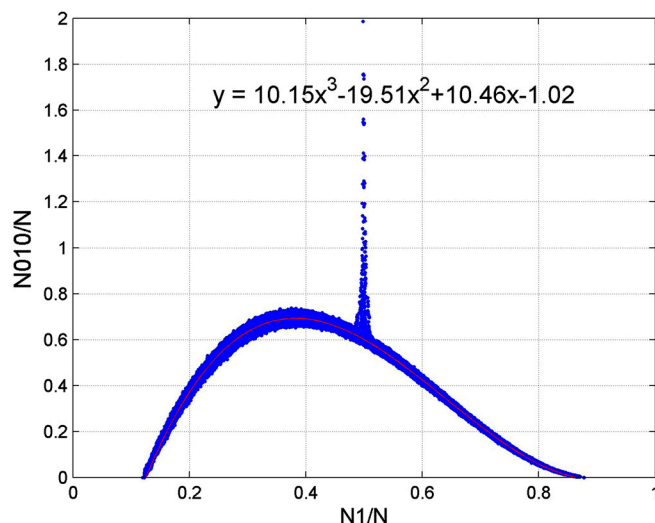


Fig. 5. Plot of N_{010}/N versus N_1/N when $\alpha = 0.5$ in the rewiring-to-random case. All simulations start at $u = 0.5$ because multiple runs from one starting point are enough to explore all of the arch. These results are from graphs with $N = 100,000$ vertices and plotted every 10,000 steps.

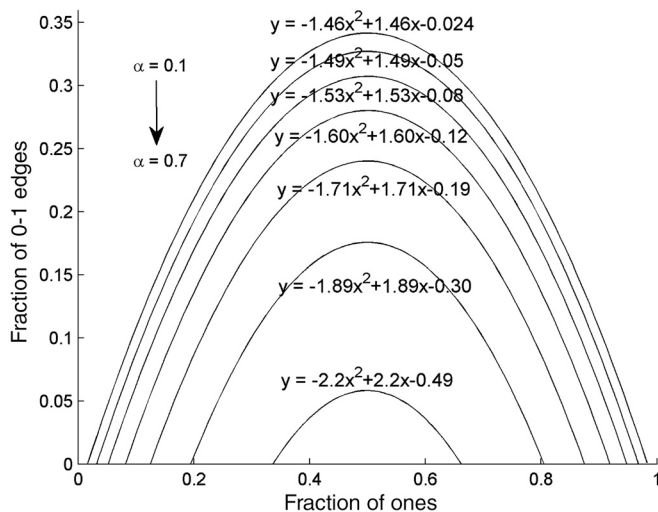


Fig. 6. Observed arches for the rewire-to-random model. The specified parabolas are fits to simulation data with $N = 10,000$, $\lambda = 4$.

N for large graphs). Fig. 7 visualizes a network shortly before this “graph fission” for $\alpha = 0.65$.

Though the nature of the phase transition looks different in the rewire-to-same model, the underlying picture is the same. Fig. 8 shows arches computed from simulations for the rewire-to-same model that correspond to the ones in Fig. 6 for the rewire-to-random model. However, now all the arches have the same support interval, $(0,1)$, and the formulas in that figure show that the curves are well approximated by $c_\alpha u(1-u)$ for different values of c_α .

In the rewire-to-same case, Vazquez et al. (40) noticed that the fraction of active links N_{10}/M plotted versus the fraction of ones converged rapidly to an arch and then diffused along it (see ref. 40, figure 4). However, they did not formulate the following:

Conjecture 2. *In the rewire-to-same model, the behavior is as described in Conjecture 1 but now $b_\alpha = 0$, so α_c is independent of the initial density u , and for $\alpha < \alpha_c$ $\rho \approx 0$.*

Approximate Calculations

Our next question is why is there a difference in the behavior of the support intervals of the arches in the two models? Consider first the rewire-to-random model. By considering all of the possible changes, one can write differential equations for the graph statistics. For example,

$$\frac{dN_{10}}{dt} = -(2-\alpha)N_{10} + (1-\alpha)[N_{100} - N_{010} + N_{110} - N_{101}].$$

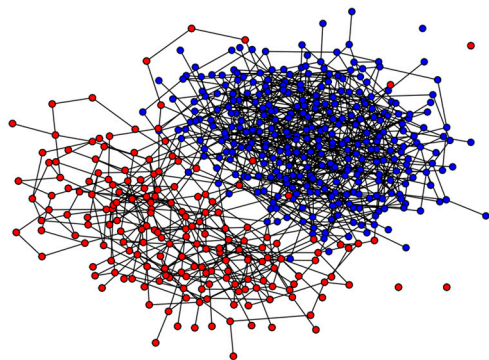


Fig. 7. Visualization of the rewire-to-random model soon before fission occurs, for $N = 500$ nodes, average degree $\lambda = 4$, and $\alpha = 0.65$. Colors correspond to the two opinions.

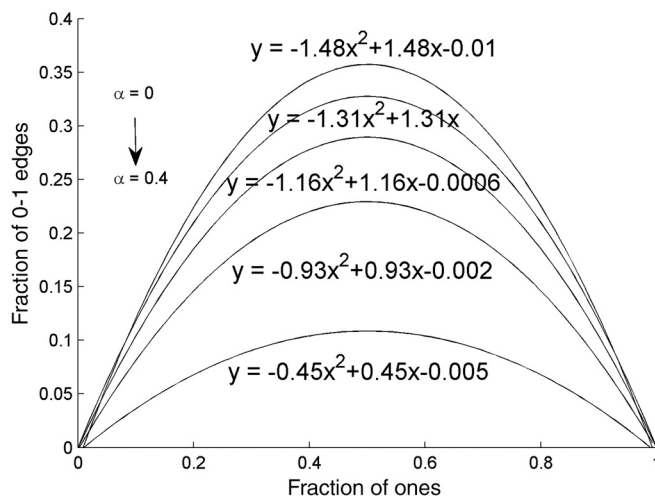


Fig. 8. Observed arches for rewire-to-same model. The specified parabolas are fits to simulation data with $N = 10,000$, $\lambda = 4$.

To be mathematically precise, for any $T < \infty$ this holds for $t \leq T$ in the limit as the number of vertices tends to ∞ . Thus these equations describe the initial behavior (i.e., as the evolving voter model converges to the arch of quasi-stationary distributions) and their equilibria as a function of u describe the arch itself.

Note that the derivatives of the two-vertex quantities N_{ij} involve two or three vertices. Derivatives of three-vertex quantities involve up to four vertices. To be able to solve the equations, we need some approximation to close the equations. In physics and ecology (see ref. 47 and references therein), it is common to use the pair approximation (PA), which in essence assumes the equilibrium state is a Markov chain: $N_{100} = N_{10}N_{00}/N_0$. A little algebra then shows (see *SI Materials* for more details about the results in this section) that, for $u \in (0,1/2]$,

$$\alpha_c(u) = \frac{\lambda - 1}{\lambda - 1 + u^2 + (1-u)^2}. \quad [1]$$

When $\lambda = 4$, $\alpha_c(1/2) = 6/7$ and $\alpha_c(u) \rightarrow 3/4$ as $u \rightarrow 0$, so the predicted fraction ρ with the minority opinion at the end rises from zero to one-half on $[3/4, 6/7]$. Fig. 9 compares the predicted value of ρ with simulations in Fig. 2 and shows the agreement is very poor.

One gets much better estimates of ρ from the approximate master equation (AME) framework introduced in ref. 48 to analyze binary state dynamics such as epidemic models. Here we follow the approach in refs. 49. Let $S_{k,m}(t)$ [$I_{k,m}(t)$] be the number of nodes at time t that are in state 0 (susceptible) [in state 1 (infected)], have degree k , and have m neighbors in state 1.

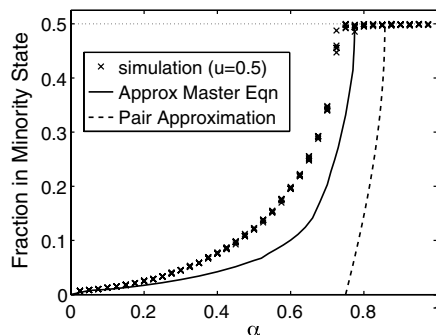


Fig. 9. Predictions of the ending minority fraction $\rho(\alpha)$ in rewire-to-random case from pair approximation (dashed line) and approximate master equation (solid line), compared with simulation (x).

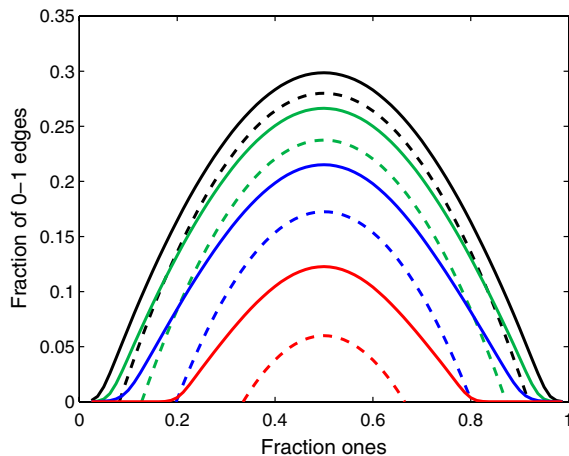


Fig. 10. Arches computed by approximate master equation (solid lines) versus simulation (dashes) for rewiring-to-random model with $\alpha = 0.4, 0.5, 0.6, 0.7$. The curves decrease as α increases.

To describe the logic behind the AME, let x be a vertex and let y be one of its neighboring vertices. Three types of things can happen: (i) rewiring may break the connection between x and y or bring a new edge to connect to x ; (ii) x or y may influence the other by a voting step; or (iii) the opinion of y may be changed by imitating one of its neighbors $z \neq x$.

Exact equations can be written for the first two types of events in terms of $\bar{S}_{k,m}$ and $\bar{I}_{k,m}$, but the third type requires an approximation. For example, if x and y are both in state 0, we postulate that y changes from zero to one at rate N_{001}/N_{00} , the expected number of 1 neighbors of a 0-0 edge. This reasoning is similar to the PA, but now we do not suppose that $N_{001}/N_{00} = N_{01}/N_0$, which, if numerical results are accurate, approximates the ratio of two cubic by a quadratic over the density u . Instead, we use identities such as

$$\sum_{k,m} (k-m) m \bar{S}_{k,m} = N_{001} \quad \text{and} \quad \sum_{k,m} m \bar{S}_{k,m} = N_{01}$$

to compute the evolution of N_{001}/N_{00} and other similar terms. As shown in Fig. 10, the AME gives a better approximation of the final minority fraction ρ than the PA. More importantly, the AME gives the correct qualitative behavior: the predicted $\rho(\alpha) > 0$ for all $\alpha > 0$ and tends to zero as $\alpha \rightarrow 0$.

One can repeat the analysis described above for the rewiring-to-same model. Using the PA, we conclude that $\alpha_c = (\lambda - 1)/\lambda$ and the arches $N_{10}/N = u(1-u)[\lambda - 1/(1-\alpha)]$ always span (0,1). This qualitative behavior agrees with Fig. 8, but the PA estimate of $\alpha_c = 3/4$ when $\lambda = 4$ drastically overestimates the value $\alpha_c \approx 0.43$ that comes from simulation (see Fig. 1). Again, one can numerically solve differential equations to employ the AME. The computed arches span (0,1) but the numerical predictions of ρ and the estimate of α_c are more accurate. See [SI Materials](#) for details of the application of the PA and AME to both models.

Discussion

We have considered a model in which the opinions of individuals and network structure coevolve. Based on a combination of simulation and approximate calculations we conclude that (i) there is a discontinuous transition in the rewiring-to-same model, similar to that in Holme and Newman (38), which occurs at an α_c independent of the initial fraction u of ones; and (ii) there is a continuous transition in the rewiring-to-random model at the critical value $\alpha_c(u)$ that depends on u , and the curves for the final fraction $\rho(\alpha, u)$ of voters in the minority agree with $\rho(\alpha, 1/2)$ for $\alpha < \alpha_c(u)$.

Thus, a small change in the dynamics of the model results in a large change in the qualitative behavior and in a manner that we find counterintuitive. One would think that the rewiring-to-same dynamic would result in a more rapid division of the population into two noninteracting groups with different opinions. The critical value for the amount of rewiring α_c needed to produce rapid disconnection is smaller in the rewiring-to-same case than $\alpha_c(1/2)$ for the rewiring-to-random. Moreover, in the rewiring-to-same case, the size of the minority opinion shrinks to almost zero for $\alpha < \alpha_c$, whereas in the rewiring-to-random case, the group fissions into two, leaving a significant minority group.

Calculations based on the approximate master equation reproduce the qualitative behavior of the phase transition. However, it would be nice to derive results directly from the exact differential equations and in a way that gives some insight into the mechanisms underlying the differences between the two models.

ACKNOWLEDGMENTS. The authors thank Raissa D'Souza, Eric Kolaczyk, Tom Liggett, and Mason Porter for their many helpful suggestions. This work began during the 2010–2011 program on Complex Networks at the Statistical and Applied Mathematical Sciences Institute. This work was partially supported by National Science Foundation Grants DMS-1005470 (to R.D.) and DMS-0645369 (to P.J.M.), by Science Foundation Ireland Grants 06/IN.1/1366, and Mathematics Applications Consortium for Science and Industry 06/MI/005 (to J.P.G.), and by the Research and Policy for Infectious Disease Dynamics program at National Institutes of Health (A.L.L.).

- Barabási AL, Albert R (2002) Statistical mechanics of complex networks. *Rev Mod Phys* 74:47–97.
- Dorogovtsev SN, Mendes JFF (2002) Evolution of networks. *Adv Phys* 51:1079–1187.
- Newman MEJ, Barabási AL, Watts DJ (2006) *The Structure and Dynamics of Networks* (Princeton Univ Press, Princeton).
- Caldarelli G (2007) *Scale-Free Networks: Complex Webs in Nature and Technology* (Oxford Univ Press, Oxford).
- Cohen R, Havlin S (2010) *Complex Networks: Structure, Robustness, and Function* (Oxford Univ Press, Oxford).
- Barrat A, Barthélemy M, Vespignani A (2008) *Dynamical Processes on Complex Networks* (Oxford Univ Press, Oxford).
- Newman MEJ (2002) Spread of epidemic disease on networks. *Phys Rev E Stat Nonlin Soft Matter Phys* 66:016128.
- Volz E (2008) SIR dynamics in random networks with heterogeneous connectivity. *J Math Biol* 56:293–310.
- Miller JC (2011) A note on a paper by Erik Volz: SIR dynamics in random networks. *J Math Biol* 62:349–358.
- Newman MEJ (2010) *Networks: An Introduction* (Oxford Univ Press, Oxford).
- Sood V, Redner S (2005) Voter model on heterogeneous graphs. *Phys Rev Lett* 94:178701.
- Durrett R (2008) *Random Graph Dynamics* (Cambridge Univ Press, Cambridge, UK).
- Castellano C, Fortunato S, Loreto V (2009) Statistical physics of social dynamics. *Rev Mod Phys* 81:591–646.
- Watts DJ (2002) A simple model of global cascades on random networks. *Proc Natl Acad Sci USA* 99:5766–5771.
- Gleeson JP, Cahalane DJ (2007) Seed size strongly affects cascades on random networks. *Phys Rev E Stat Nonlin Soft Matter Phys* 75:056103.
- Montanari A, Saberi A (2010) The spread of innovations in social networks. *Proc Natl Acad Sci USA* 107:20196–20201.
- Ohtsuki H, Hauert C, Lieberman E, Nowak MA (2006) A simple rule for the evolution of cooperation on graphs and social networks. *Nature* 441:502–505.
- Easley D, Kleinberg J (2010) *Networks, Crowds and Markets* (Oxford Univ Press, Oxford).
- Gross T, Blasius B (2008) Adaptive coevolutionary networks: A review. *J R Soc Interface* 5:259–271.
- Skyrms B, Pemantle R (2000) A dynamic model of social network formation. *Proc Natl Acad Sci USA* 97:9340–9346.
- Ebel H, Bornholdt S (2002) Co-evolutionary games on networks. *Phys Rev E Stat Nonlin Soft Matter Phys* 66:056118.
- Zimmerman MG, Eguiluz VM, San Miguel M (2004) Coevolution of dynamical states and interactions on networks. *Phys Rev E Stat Nonlin Soft Matter Phys* 69:065102.
- Zimmerman MG, Eguiluz VM (2005) Cooperation, social networks, and the emergence of leadership in a prisoner's dilemma game. *Phys Rev E Stat Nonlin Soft Matter Phys* 72:056118.
- Santos FC, Pacheco JM, Lenaerts T (2006) Cooperation prevails when individuals adjust their social ties. *PLoS Comput Biol* 2:e140.
- Volz E, Meyers LA (2007) Susceptible-infected recovered epidemics in dynamic contact networks. *Proc Biol Sci* 274:2925–2933.
- Volz E, Meyers LA (2009) Epidemic thresholds in dynamic contact networks. *J R Soc Interface* 6:233–241.
- Gross T, Dommar D'Lima CJ, Blasius B (2006) Epidemic dynamics on an adaptive network. *Phys Rev Lett* 96:208701.
- Zanette DH (2007) Coevolution of agents and networks in an epidemiological model. *arXiv:0707.1249*.

29. van Segroeck S, Santos FC, Pacheco JM (2010) Adaptive contact networks change effective disease infectiousness and dynamics. *PLoS Comput Biol* 6:e1000895.
30. Gil S, Zanette DH (2006) Coevolution of agents and opinions: Opinion spreading and community disconnection. *Phys Lett A* 356:89–94.
31. Zanette DH, Gil S (2006) Opinion spreading and agent segregation on evolving networks. *Physica D* 224:156–165.
32. Pacheco JM, Traulsen A, Nowak MA (2006) Coevolution of strategy and structure in complex networks with dynamical linking. *Phys Rev Lett* 97:258103.
33. Kozma B, Barrat A (2008) Consensus formation on adaptive networks. *Phys Rev E Stat Nonlin Soft Matter Phys* 77:016102.
34. Kozma B, Barrat A (2008) Consensus formation on coevolving networks: Groups' formation and structure. *J Phys A Math Gen* 41:224020.
35. Iniguez G, Kertész J, Kaksi KK, Barrio RA (2009) Opinion and community formation in coevolving networks. *Phys Rev E Stat Nonlin Soft Matter Phys* 80:066119.
36. Macy MV, Kitts JA, Flache A (2003) Polarization of dynamic networks. *Dynamic Social Network Modeling and Analysis* (Natl Acad Press, Washington, DC), pp 162–173.
37. Henry AD, Pralat P, Zhang CQ (2011) Emergence of segregation in evolving social networks. *Proc Natl Acad Sci USA* 108:8605–8610.
38. Holme P, Newman MEJ (2006) Nonequilibrium phase transition in the coevolution of networks and opinions. *Phys Rev E Stat Nonlin Soft Matter Phys* 74:056108.
39. Kimura D, Hayakawa Y (2008) Coevolutionary networks with homophily and heterophily. *Phys Rev E Stat Nonlin Soft Matter Phys* 78:016103.
40. Vazquez F, Eguíluz VM, San Miguel MS (2008) Generic absorbing transition in coevolution dynamics. *Phys Rev Lett* 100:108702.
41. Herrera JL, Cosenza MG, Tucci K, González-Avella JC (2011) General coevolution of topology and dynamics in networks. arXiv:1102.3647.
42. Durrett R (2010) *Probability: Theory and Examples* (Cambridge Univ Press, Cambridge, UK), 4th Ed.
43. Holley RA, Liggett TM (1976) Ergodic theorems for weakly interacting systems and the voter model. *Ann Probab* 4:195–228.
44. Liggett TM (1999) *Stochastic Interacting Systems: Contact, Voter and Exclusion Processes* (Springer, New York), pp 139–145.
45. Cox JT, Greven A (1990) On the long term behavior of some finite particle systems. *Probab Theory Rel Fields* 85:195–237.
46. Borgs C, Chayes JT, Lovász L, Sós VT, Vesztegombi K (2008) Convergent sequences of dense graphs. I. Subgraph frequencies, metric properties and testing. *Adv Math* 219:1801–1851.
47. Ellner SP (2001) Pair approximation for lattice models with multiple interaction scales. *J Theor Biol* 210:435–447.
48. Marceau V, Noël P-A, Hébert-Dufresne L, Allard A, Dubé L (2010) Adaptive networks: Coevolution of disease and topology. *Phys Rev E Stat Nonlin Soft Matter Phys* 82:036116.
49. Gleeson JP (2011) High-accuracy approximation of binary-state dynamics on networks. *Phys Rev Lett* 107:068701 extended version arXiv:1104.1537.

Supporting Information

Durrett et al. 10.1073/pnas.1200709109

SI Methods

Notation. N_1 is the number of vertices in state 1. N_{ij} is the number of oriented $i-j$ edges, so $N_{10} = N_{01}$ and N_{11} counts each unoriented 1-1 edge twice. N_{ijk} is the number of oriented triples $x-y-z$ having states i, j, k . For symmetric strings such as 0-1-0, all instances are counted twice. The fact that this notation is more natural than dividing by 2 to eliminate overcounting, can be seen by observing that, if $d(x)$ is the degree of x ,

$$\sum_{ij} N_{ij} = \sum_x d(x) \quad \sum_{ijk} N_{ijk} = \sum_x d(x)[d(x) - 1].$$

Differential Equations. Consider first the rewired-to-random model and let $u = N_1/N$ be the initial fraction of vertices in state 1. By considering all of the possible changes, one arrives at the following differential equations:

$$\begin{aligned} \frac{dN_{10}}{dt} &= -(2 - \alpha)N_{10} + (1 - \alpha)[N_{100} - N_{010} + N_{110} - N_{101}] \\ \frac{1}{2} \frac{dN_{11}}{dt} &= [1 - \alpha(1 - u)]N_{10} + (1 - \alpha)[N_{101} - N_{011}] \\ \frac{1}{2} \frac{dN_{00}}{dt} &= (1 - \alpha u)N_{10} + (1 - \alpha)[N_{010} - N_{100}]. \end{aligned} \quad [\text{S1}]$$

Here we have used the fact that in the initial phase modeled by these differential equations $N_1 \approx Nu$ and $N_0 \approx N(1 - u)$. We have $N_{11} + 2N_{10} + N_{00} = M$, so the sum of the three differential equations is zero.

Rewire-to-Random Model, Pair Approximation. The calculations presented here were inspired by similar equations in Kimura and Hayakawa (1). Omitting the first equation from [S1], which is redundant,

$$\begin{aligned} \frac{1}{2} \frac{dN_{11}}{dt} &= [1 - \alpha(1 - u)]N_{10} + (1 - \alpha)[N_{101} - N_{011}], \\ \frac{1}{2} \frac{dN_{00}}{dt} &= (1 - \alpha u)N_{10} + (1 - \alpha)[N_{010} - N_{100}]. \end{aligned}$$

Using these two equations and the pair approximation,

$$\begin{aligned} \frac{[1 - \alpha(1 - u)]}{1 - \alpha} N_{10} &= \frac{N_{01}N_{11}}{uN} - \frac{N_{10}N_{01}}{(1 - u)N} \\ \frac{(1 - \alpha u)}{1 - \alpha} N_{10} &= \frac{N_{10}N_{00}}{(1 - u)N} - \frac{N_{01}N_{10}}{uN}, \end{aligned}$$

which leads to the equations

$$\frac{N_{11}}{uN} - \frac{N_{10}}{(1 - u)N} = 1 + \frac{\alpha u}{1 - \alpha} \quad [\text{S2}]$$

and

$$\frac{N_{00}}{(1 - u)N} - \frac{N_{10}}{uN} = 1 + \frac{\alpha(1 - u)}{1 - \alpha}. \quad [\text{S3}]$$

Adding uN times [S2] to $(1 - u)N$ times [S3], we have

$$N_{11} + N_{00} - \left(\frac{u}{1 - u} + \frac{1 - u}{u} \right) N_{01} = \left[1 + \frac{[u^2 + (1 - u)^2]\alpha}{1 - \alpha} \right] N. \quad [\text{S4}]$$

When $N_{01} = 0$, we have $N_{11} + N_{00} = \lambda N$ and solving gives

$$\alpha_c(u) = \frac{\lambda - 1}{\lambda - 1 + u^2 + (1 - u)^2}.$$

When $u = 1/2$ and $\lambda = 4$, we get $\alpha_c = 3/3.5 = 6/7$. As $u \rightarrow 0$, $\alpha_c(u) \rightarrow (\lambda - 1)/\lambda = 3/4$.

Similarly, using [S4] with $N_{11} + N_{00} = \lambda N - 2N_{01}$ we have

$$\lambda N - 2N_{01} - \left(\frac{u}{1 - u} + \frac{1 - u}{u} \right) N_{01} = \left[1 + \frac{[u^2 + (1 - u)^2]\alpha}{1 - \alpha} \right] N. \quad [\text{S5}]$$

A little algebra gives

$$2 + \frac{u}{1 - u} + \frac{1 - u}{u} = \frac{2u - 2u^2 + u^2 + 1 - 2u + u^2}{u(1 - u)} = \frac{1}{u(1 - u)}. \quad [\text{S6}]$$

Rearranging [S5] and using [S6] gives

$$\left(\lambda - 1 - \frac{[u^2 + (1 - u)^2]\alpha}{1 - \alpha} \right) N = \frac{1}{u(1 - u)} N_{01},$$

and solving we get the pair approximation for the arch:

$$\frac{N_{01}}{N} = u(1 - u) \left(\lambda - 1 - \frac{[u^2 + (1 - u)^2]\alpha}{1 - \alpha} \right).$$

Note that, as α decreases from $\alpha_c(1/2) = (\lambda - 1)/(\lambda - 1/2)$ to $(\lambda - 1)/\lambda$, the arch expands from a point to a curve that spans $(0, 1)$.

Rewire-to-Same Model, Pair Approximation. In this case, the differential equations are

$$\begin{aligned} \frac{1}{2} \frac{dN_{11}}{dt} &= N_{10} + (1 - \alpha)[N_{101} - N_{011}], \\ \frac{1}{2} \frac{dN_{00}}{dt} &= N_{10} + (1 - \alpha)[N_{010} - N_{100}]. \end{aligned}$$

Using these equations and the pair approximation as before,

$$\begin{aligned} \frac{1}{1 - \alpha} N_{10} &= \frac{N_{01}N_{11}}{uN} - \frac{N_{10}N_{01}}{(1 - u)N} \\ \frac{1}{1 - \alpha} N_{10} &= \frac{N_{10}N_{00}}{(1 - u)N} - \frac{N_{01}N_{10}}{uN}, \end{aligned}$$

which leads to the equations

$$\frac{N_{11}}{uN} - \frac{N_{10}}{(1 - u)N} = \frac{1}{1 - \alpha} \quad [\text{S7}]$$

and

$$\frac{N_{00}}{(1-u)N} - \frac{N_{10}}{uN} = \frac{1}{1-\alpha}. \quad [\text{S8}]$$

Adding uN times the first to $(1-u)N$ times the second, we have

$$N_{11} + N_{00} - \left(\frac{u}{1-u} + \frac{1-u}{u} \right) N_{01} = \frac{N}{1-\alpha}. \quad [\text{S9}]$$

When $N_{01} = 0$, we have $N_{11} + N_{00} = \lambda N$, giving $1 - \alpha_c = 1/\lambda$ or

$$\alpha_c = 1 - \frac{1}{\lambda} = \frac{\lambda - 1}{\lambda}.$$

Using [S9] with $N_{11} + N_{00} = \lambda N - 2N_{01}$ and the algebra in [S6] yields

$$[\lambda - (1-\alpha)^{-1}]N = \frac{N_{01}}{u(1-u)}$$

and the following approximation for the arch

$$\frac{N_{01}}{N} = u(1-u) \left(\lambda - \frac{1}{1-\alpha} \right).$$

Approximate Master Equations

Rewire-to-Random Version. The approximate master equation for the susceptible sites is

$$\begin{aligned} \frac{d}{dt} \bar{S}_{k,m} = & \alpha \{ -(2-u)m\bar{S}_{k,m} + (1-u)(m+1)\bar{S}_{k,m+1} \\ & + (m+1)\bar{S}_{k+1,m+1} \} \\ & + \alpha N_{01} [-2\bar{S}_{k,m} + \bar{S}_{k-1,m-1} + \bar{S}_{k-1,m}] / N \\ & + (1-\alpha) [-m\bar{S}_{k,m} + (k-m)\bar{I}_{k,m}] \\ & + (1-\alpha) [-\beta^S(k-m)\bar{S}_{k,m} + \beta^S(k-m+1)\bar{S}_{k,m-1} \\ & - \gamma^S m\bar{S}_{k,m} + \gamma^S(m+1)\bar{S}_{k,m+1}], \end{aligned} \quad [\text{S10}]$$

where

1. Kimura D, Hayakawa Y (2008) Coevolutionary networks with homophily and heterophily. *Phys Rev E Stat Nonlin Soft Matter Phys* 78:016103

$$\begin{aligned} \beta^S &= \frac{\sum_{k,m} (k-m)m\bar{S}_{k,m}}{\sum_{k,m} (k-m)\bar{S}_{k,m}} = \frac{N_{001}}{N_{00}} \\ \gamma^S &= \frac{\sum_{k,m} (k-m)^2 \bar{I}_{k,m}}{\sum_{k,m} (k-m)\bar{I}_{k,m}} = \frac{N_{010}}{N_{01}} + 1. \end{aligned}$$

Here β^S gives the expected number of 1 neighbors of a 0-0 edge. For a vertex in state 0 with j neighbors in state 0, the number of oriented 0-1-0 containing it is $j(j-1)$. Thus, N_{010}/N_{01} gives the expected number of zero neighbors of the 1 at the end of a 0-1 edge, and the +1 in the definition of γ^S counts the zero on the conditioning edge.

The approximations for the arches reported in Fig. 10 in the main text are obtained by numerically solving the system to steady state. Mathematica's NDSolve function was used starting with a Poisson degree distribution of mean degree $\lambda = 4$, vertices independently assigned the value 1 with probability u , and the equations cut off at maximum degree $K = 15$ (The results are not appreciably affected by increasing K .)

Rewire to Same. The voter terms are exactly as in the rewire-to-random case, whereas the number of possibilities for rewiring is reduced:

$$\begin{aligned} \frac{d}{dt} \bar{S}_{k,m} = & \alpha \{ -2m\bar{S}_{k,m} + (m+1)\bar{S}_{k+1,m+1} + (m+1)\bar{S}_{k,m+1} \} \\ & + \alpha N_{01} [-\bar{S}_{k,m} + \bar{S}_{k-1,m}] / [N(1-u)] \\ & + (1-\alpha) [-m\bar{S}_{k,m} + (k-m)\bar{I}_{k,m}] \\ & + (1-\alpha) [-\beta^S(k-m)\bar{S}_{k,m} + \beta^S(k-m+1)\bar{S}_{k,m-1} \\ & - \gamma^S m\bar{S}_{k,m} + \gamma^S(m+1)\bar{S}_{k,m+1}]. \end{aligned} \quad [\text{S11}]$$

Again we generate our predictions by numerically solving the differential equations. When $\lambda = 4$, the predictions for the arch are given in Fig. S1.

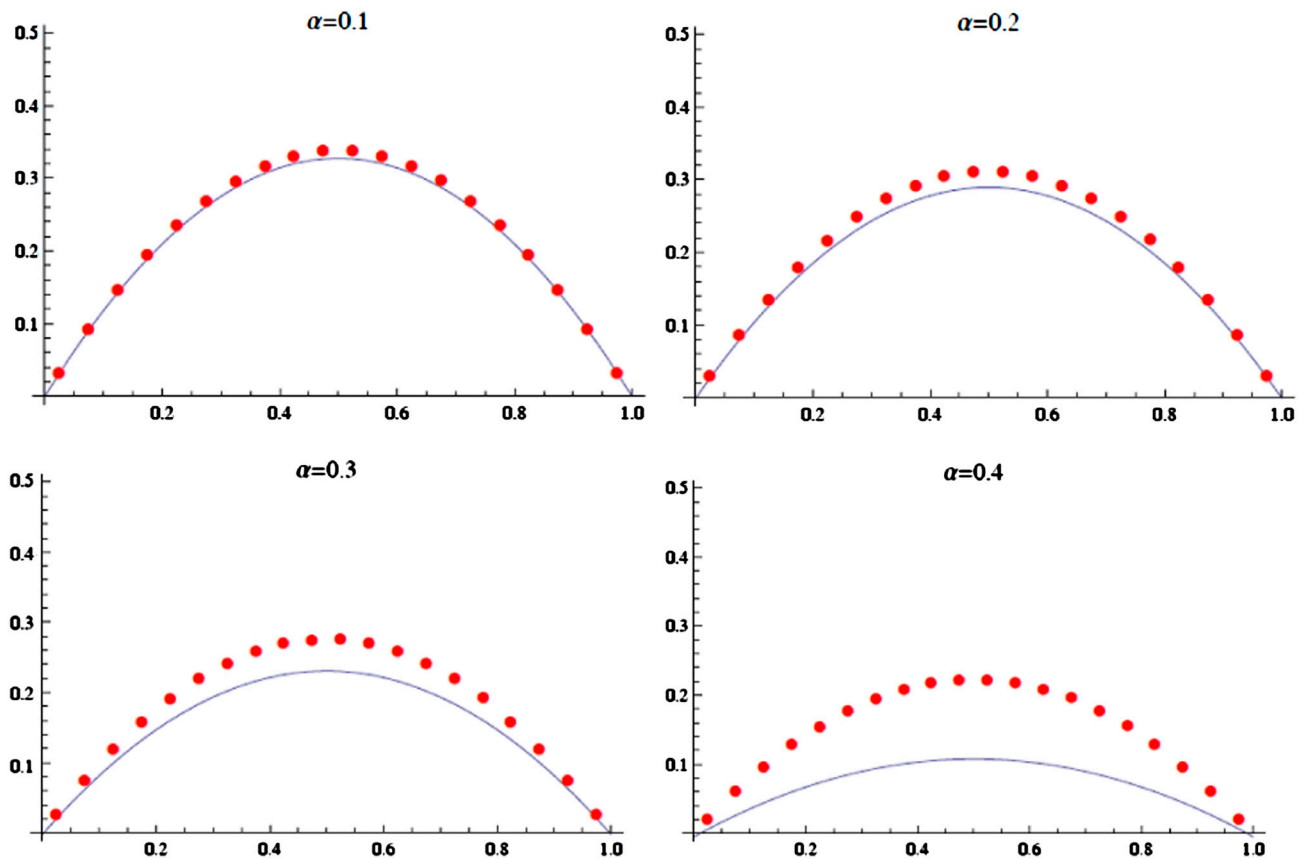


Fig. S1. Arches computed by the approximate master equation (dots) compared to rewire-to-same compared to simulations (solid lines) for the indicated values of α .